

## Fabrication of low power micro-heater for micro-gas sensor

### II. Characteristics of micro-gas sensor

Wan-Young Chung\*, Sang-Moon Lee\*\*, Bong-Hwi Kang\*\*, Dong-Kun Jang\*\*\*,  
Duk-Dong Lee\*\*, and Noboru Yamazoe\*\*\*\*

#### Abstract

A new planar-type microsensor, which had a platinum heater and a sensing layer on the same plane was fabricated on silicon substrate with stress-relieved PSG(phosphosilicate glass)/Si<sub>3</sub>N<sub>4</sub>(800nm/150nm) diaphragm. The proposed planar-type microsensor could be fabricated by simple silicon process using only 3 masks for photolithography process compared with 5 or 6 masks of the typical micro-gas sensor. The thermal properties of the microsensor from thermal simulation were compared with those of the fabricated microheater. Although there are some discrepancy between the simulation result and the result from the fabricated microheater, the thermal simulation by FEM was proved to be an useful method to evaluate the thermal properties of microheater. The sensing characteristics of the fabricated microsensor with the planar-type heater were investigated also.

#### I. Introduction

Most metal-oxide gas sensors for detecting hydrocarbon or combustible gases work at high temperatures between 100 and 400°C in order to operate efficiently and be adequately sensitive to gases<sup>[1]</sup>. This implies rigid restrictions on the available technologies. Therefore in-situ heating is one of the basic requirements for a micro-gas sensor to maintain it at the elevated temperature with low power consumption.

For low power consumption and good thermal isolation from the surrounding circuits, the microheater of the sensor has to be mounted on a thermal insulation layer. Until now, two kinds of membrane-type structures were widely used for thermal insulation. One structure uses the substrate silicon removed by etching from the back side<sup>[2-4]</sup> and the other uses the substrate silicon removed by etching from the front side, that is, micro-bridge structure<sup>[5-7]</sup>. Among both structures, the former structure was more frequently used due to easy fabrication process and mechanical strength.

Recently, we have reported research on thermal distribution analyses of the platinum microheater with PSG/Si<sub>3</sub>N<sub>4</sub> diaphragm. The simulations were performed by using a commercially available finite element method(FEM) package<sup>[8]</sup>. In the report,

\* Dept. of Electronic Engineering, Semyung Univ.

\*\* School of Electronic & Electrical Engineering, Kyungpook National University

\*\*\* Semiconductor R&D Center, KEC

\*\*\*\* Dept. of Materials Science and Technology, Kyushu University, Japan

※ This paper was supported in part by NON DIRECTED RESEARCH FUND, Korea Research Foundation, 1995.

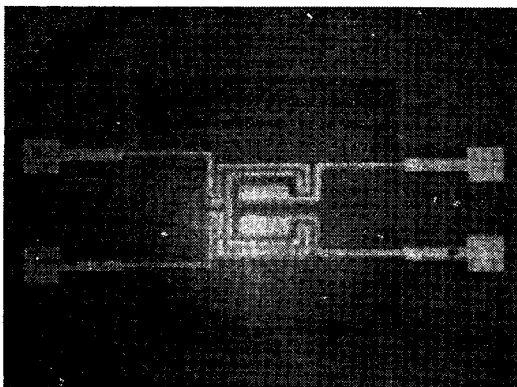
<접수일자 : 1997년 1월 14일>

two kinds of micro-gas sensors, the planar-type structure, which has a heater and a sensing layer on the same plane, and the stack-type structure, which has the stacked structure of sensing layer/insulator/heater, were designed. The thermal analyses including temperature distribution over the diaphragm and power consumption of the heater were compared with each other. From the simulation result, we concluded that the planar-type heater consumed about 10% more power than the stack-type heater for the same operating temperature of sensing layer. The temperature uniformity over the sensing layer was, however, relatively good in the planar-type heater compared with in the stack-type heater. First of all, the planar-type heater proposed in this study could be fabricated by only 3-masks compared with 5 or 6-masks of the stack-type heater.

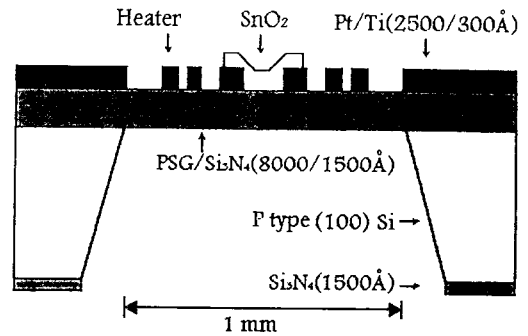
In this study, the simulated micro-heater, the planar structure, was fabricated. The heating properties of the heater were compared with the results of simulation and the CO gas sensing characteristics of the microsensor with the heater were investigated.

## II. Device Fabrication

The structure of a proposed planar-type microsensor is shown in Fig.1. The dimensions of



(a)



(b)

Fig. 1. The structure of a planar-type microsensor. (a) SEM of over view (b) Schematic cross sectional view

the sensitive tin oxide film were  $260 \mu\text{m} \times 260 \mu\text{m}$ , those of the square diaphragm were  $1.5 \text{ mm} \times 1.5 \text{ mm}$  and those of the fabricated whole silicon chip were  $3.7 \text{ mm} \times 3.7 \text{ mm}$ .

A double-side polished p-type(100) silicon wafer with a thickness of  $320 \mu\text{m}$  and a resistivity of  $10 \sim 20 \Omega \cdot \text{cm}$  was used as a substrate. However, a stress-relieved dielectric layer<sup>[9]</sup>, composed of a low-pressure chemical-vapor-deposited(LPCVD) silicon nitride(150 nm) and atmosphere-pressure chemical-vapor-deposited (APCVD) phosphorous silica glass(PSG, 800 nm), is used as a membrane on the front side and as a passivation layer during back etching on the backside. Figure 2 shows flow sequence of fabrication process for the planar-type microsensor. The process steps were as follows:

(1) A 230 nm thin film of Pt with 30 nm Ti as adhesion layer was deposited by r.f. magnetron sputtering.

(2) The PSG/Si<sub>3</sub>N<sub>4</sub> layer of backside was patterned by wet etching and reactive ion etching(RIE) subsequently using Mask I, and the Pt/Ti layer of front side was patterned using Mask II by double side alignment.

(3) The Pt/Ti layer was etched to realized a resistance heater and electrode pairs for the sensing layer.

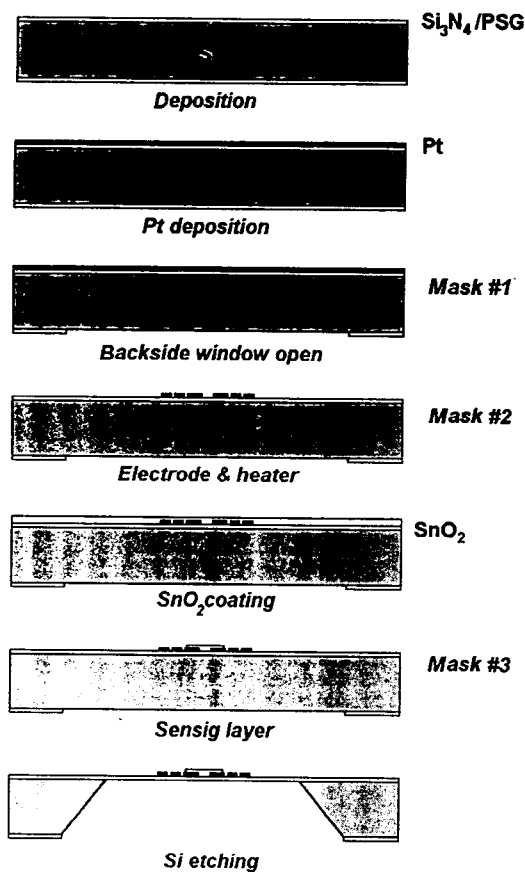


Fig. 2. The flow sequence of fabrication process for the planar-type microsensor.

(4) The  $\text{SnO}_2$  solution synthesized by hydrothermal method<sup>[9]</sup> was spin coated over the silicon substrate with platinum electrode pairs and etched to form sensing layer using Mask III, and the sensing layer was heat treated at  $600^\circ\text{C}$  for 30 min subsequently.

(5) Finally, the backside of the Si substrate was removed by anisotropic KOH etching, and subsequently thermal isolation structure with a 950 nm thick square diaphragm was fabricated.

### III. Results and Discussion

#### 3.1 Heating characteristics of the heater

The heating characteristics of the planar-type

platinum heater were examined. The platinum resistor was prepared for common use of heater and temperature sensor. The resistance of the platinum heater was measured as a function of the temperature on a hot plate in order to calibrate the temperature scale. From the relationship between temperature and resistance of the platinum resistor, the measured positive temperature coefficient (PTC) of the platinum heater was about 3500 ppm/ $^\circ\text{C}$ . It has been reported that the PTC is  $0.385 \Omega/\text{K}$ <sup>[11]</sup> for industrial platinum resistance thermometers which resistance value is  $100 \Omega$  at  $0^\circ\text{C}$ . This means that the electrical resistance raises with  $0.385 \Omega$  if the temperature increase with 1 K. The discrepancy between the measured PTC and standard PTC may be come from the facts that the thickness of the platinum resistor of the temperature sensor in this experiment is too thin to show bulk effect and the fabricated platinum resistor has some different qualities.

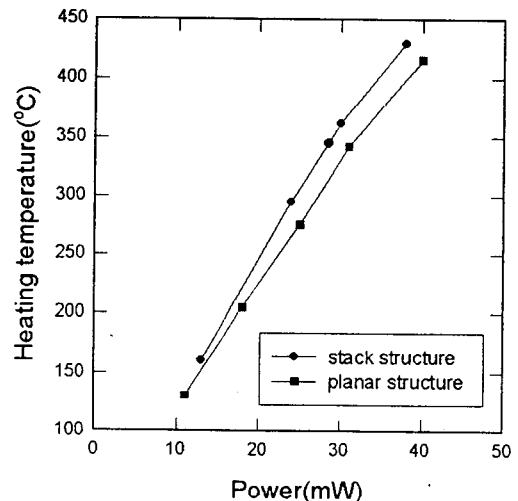


Fig. 3. Simulated heating characteristics of microheaters.

Figure 3 shows simulated heating characteristics of two types of microheaters, that is, the planar-type and the stack-type microheaters. In

the planar-type structure, the sensitive film was heated by the platinum heater on the outer side of the sensitive layer. The heating energy of the heater might be transferred in the form of thermal conductive energy. Therefore, some convection energy might be dissipated during thermal conduction from platinum heater to sensitive layer in the planar-type structure. On the other hand, in the stack-type structure with the structure of sensing layer/oxide(insulator)/heater, the sensing layer could be heated by the heater situated just below of the sensing film. Consequently, the stack-type structure could save the consuming power for the high operating temperature. The simulated power consumption of the planar-type heater for the operating temperature of 350 °C of the sensing layer was 33 mW( or 34 mW with consideration of radiation effect) and this power is about 10% more than that of the stack-type heater for the same operating temperature.

The simulated relationship between power and temperature of the sensing layer was compared with that of the fabricated microheater in Fig. 4.

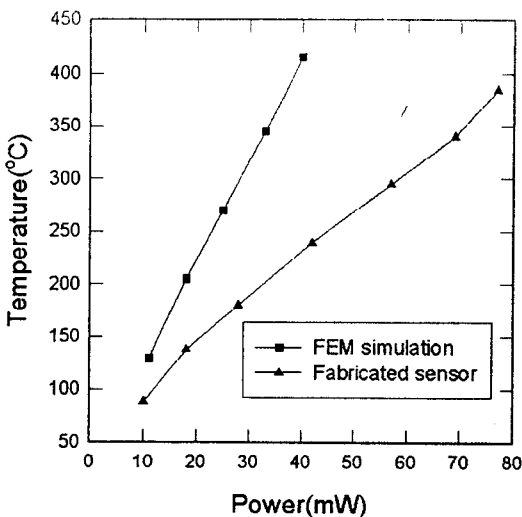


Fig. 4. The heating properties of the planar-type microsensor from the computer simulation and the fabricated microheater.

The consumed power of the planar-type heater for the operating temperature of 350 °C is about 68 mW and this is about 2 times of the simulated result. This discrepancy between the simulated result and the tested result from the fabricated microheater might come from the simplification of the simulation condition, that is, disregard of the effects of bonding pad, lead wire and touch of the silicon sample with package die.

Though there are some discrepancy between the simulation result and the result from the fabricated microheater, the computer simulation method using FEM looks very useful method to evaluate the thermal distribution and thermal consumption of the micro silicon heater.

### 3.2 Gas sensitivity characteristics of the microsensor

The most commonly used methods for the preparation of sensing film of micro-gas sensor are physical methods such as r.f. sputtering and thermal evaporation<sup>[12-14]</sup>. Though it is not easy to be compatible with microelectronic process, the chemical preparation method such as sol-gel method<sup>[10,15]</sup> and spray method<sup>[16]</sup> for the preparation of gas sensitive film has many advantages over the physical ones because of the follows: (i) catalyst can easily incorporated, (ii) additive can exactly controlled, (iii) no special apparatuses are required, (iv) the resultant films may possibly be characterized by an ultrafine and porous structure with a large specific area.

The coating SnO<sub>2</sub> and Sb-doped SnO<sub>2</sub> solutions were colloidal SnO<sub>2</sub> solution (SnO<sub>2</sub> content 8 wt.%, mean diameter of particles : about 3 nm) and SnO<sub>2</sub>(Sb) solution (SnO<sub>2</sub> content 10 wt.%, Sb content 0.6~0.7 wt.%, mean diameter of SnO<sub>2</sub> particles : about 3 nm), and these are commercially available solutions (Taki Chemical Co., Ltd., Japan). These solutions were prepared by means of the hydrothermal method described in detail elsewhere<sup>[10,15]</sup>. The mixed solution of SnO<sub>2</sub> and

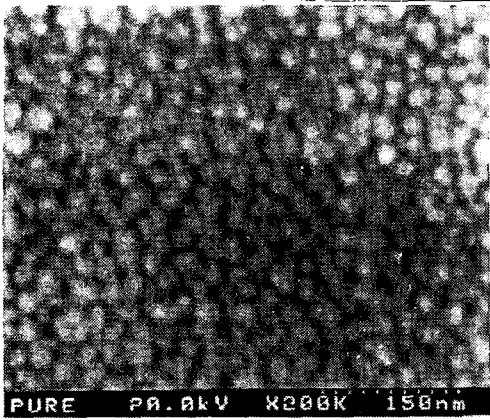
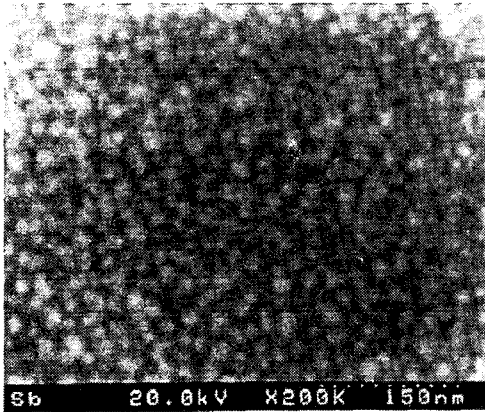
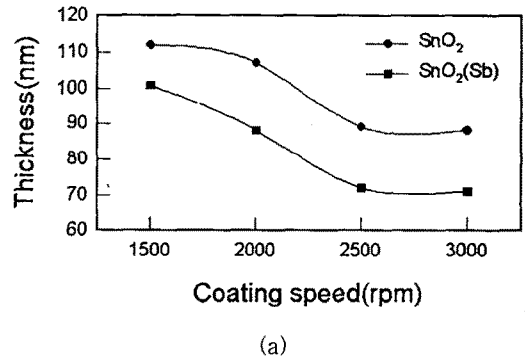
(a)  $\text{SnO}_2$  film(b)  $\text{SnO}_2(\text{Sb})$  film(c) expanded micrograph of  $\text{SnO}_2$  film

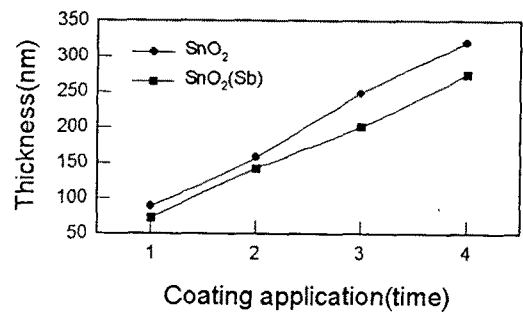
Fig. 5. High-resolution SEM micrographs of  $\text{SnO}_2$  film(a) and  $\text{SnO}_2(\text{Sb})$  film(b) spin-coated at 3000rpm and 2 times application.

$\text{SnO}_2(\text{Sb})$  was used to control the Sb contents of a coated film.

The surface morphologies were observed by high resolution SEM. Figure 5 shows the surface morphologies of  $\text{SnO}_2$  and  $\text{SnO}_2(\text{Sb})$  films, which were spin-coated at 3000 rpm, at two times and heat treated at 600 °C for 30 min in air. Figure 5(c) is the expanded micrograph of the  $\text{SnO}_2$  film in Fig.5(a). A comparison of Fig.5(a) with Fig.5(b) suggested that there are no great microstructural differences between undoped and Sb doped  $\text{SnO}_2$  films, and that the sol-gel spin-coating technique can produce homogeneous  $\text{SnO}_2$  films with crystallites very regular in size. The film was composed of very fine, below 150Å, particles of  $\text{SnO}_2$  crystallite and was well condensed flat film. And we can see that interparticle neck formation in the  $\text{SnO}_2$  film is minimal in Fig.5.



(a)

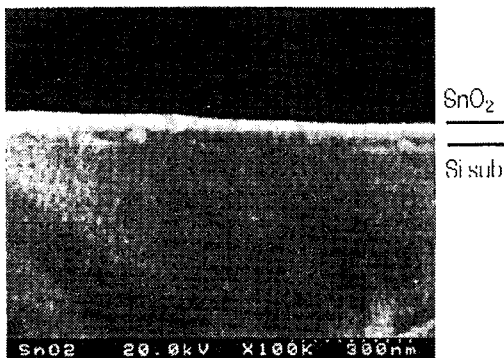


(b)

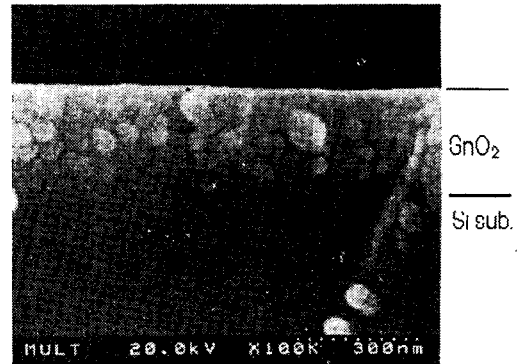
Fig. 6. Dependence of film thickness on (a) spin-speed of coating and (b) the number of coating applications.

The film thickness was controlled by spin-speed variation between 1500 rpm to 3000 rpm by step of 500 rpm and the number of coating application. The film thickness was monitored by stylus method and ellipsometer, and confirmed by cross sectional SEM view. The film thickness measured by SEM shows good agreement with the thickness values measured by stylus and ellipsometer. Figure 6 shows the relationship of SnO<sub>2</sub> and SnO<sub>2</sub>(Sb) films between the film thickness and spin-speed. Film thickness decreased with increasing spin-speed. It was also found that there was a linear relationship between the film thickness and the number of coating application. In case of SnO<sub>2</sub> film, film thickness increased with an interval of about 74 nm by increasing the number of applications from 1 to 4 at the spin-speed of 3000 rpm.

Figure 7 is typical cross sectional views of the SnO<sub>2</sub> films spin-coated at 3000 rpm on silicon substrate at 1 time and 4 times respectively. These SEM were photographed over the sample placed vertically. The thickness of the film, which was coated at a time, is about 70 nm and that of the film, which was coated at 4 times, is about 300 nm. Figure 7 indicates the primary particles(=below 15 nm diameter) form the large secondary tin oxide agglomerate(=averagely 50 nm diameter). This agglomerate may possibly make the coated film into the porous film.



(a)



(b)

Fig. 7. Cross-sectional views of spin-coated SnO<sub>2</sub> films.

Aqueous solution of hydroiodic acid(57% HI in water, 99.99%) from Aldrich Chemical Company, Inc. was used as etching solution of SnO<sub>2</sub> film. The 150 nm thick SnO<sub>2</sub> film made by sol-gel method was etched at 80 °C by photolithographic process using Posi-PR. As is shown in Fig.8, a high-resolution pattern(about 5 μm) could be realized. The etch rate was about 50 nm/min at 80 °C. The etching of SnO<sub>2</sub> films in HI gives excellent pattern resolution and the film patterned by HI solution shows no sensitivity decreasing after etching.

The gas sensitivity of microsensor to CO gas was tested to evaluate the heater operation. The gas sensitivity(S) was defined as the ratio of the resistance in air(R<sub>a</sub>) and in CO gas(R<sub>g</sub>). Figure 9

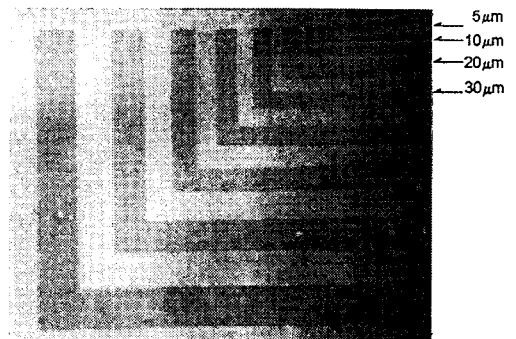


Fig. 8. Result of wet etching of SnO<sub>2</sub> film on silicon substrate.

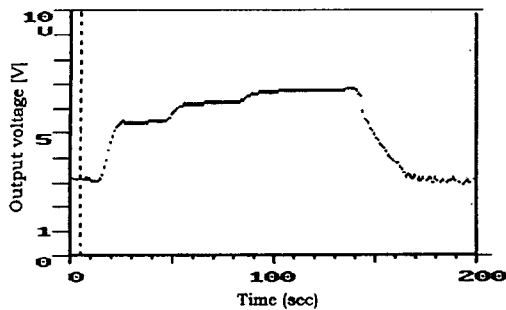


Fig. 9. Time response of the microsensor with  $\text{SnO}_2(\text{Sb} : 0.5 \text{ wt.}\%)$  film to CO gas.

shows the response characteristics of microsensor with  $\text{SnO}_2(\text{Sb} : 0.5 \text{ wt.}\%)$  film to three CO concentrations (2000, 3000 and 5000 ppm). The CO sensitivity of  $\text{SnO}_2(\text{Sb})$  film is about 4 to 2000 ppm CO gas at  $250^\circ\text{C}$  and the film shows fast response below 10 sec.

#### IV. Conclusions

Thermal properties of the two types of microheaters, the stack-type and the planar-type, were simulated by FEM commercial package and the planar-type heater was fabricated by silicon process technique. The stack-type structure with sensing layer/oxide/heater could save the power consumption for the high operating temperature. In this structure, the sensing layer could be heated by the heater situated just below of the sensing film. However, the planar-type structure with a sensing layer and a platinum heater on the same plane could be fabricated simple process using only 3 masks for photolithography process. In the planar-type structure, the sensing layer was heated by the heater situated out of the sensing film and the heating energy probably was transferred by thermal conduction mechanism of the PSG/ $\text{Si}_3\text{N}_4$  diaphragm.

The planar-type heater structure proposed in this study could be available technology for simple fabrication process and comparatively low power consumption heating.

#### V. REFERENCES

- [1] N.Yamazoe, Y.Kurokawa and T.Seiyama, "Effects of additives on semiconductor gas sensor", *Sensors and Actuators*, vol.4, pp.283-289, 1983.
- [2] N.Najapi, K.D.Wise and J.K.Schwank, "A micromachined ultra-thin-film gas detector", *IEEE Transaction on Electron Devices*, vol.41, no.10, pp.1770-1777, 1994.
- [3] W.-Y.Chung, C.-H. Shim, S.-D. Choi and D.-D.Lee, Tin oxide microsensor for LPG monitoring, *Sensors and Actuators B*, vol.20, pp.139-143, 1994.
- [4] D.-D.Lee, W.-Y.Chung, M.-S.Choi, J.-M. Baek, Low power micro gas sensor, *Sensors and Actuators B*, vol.33, pp.147-150, 1996.
- [5] J.S.Suehle, R.E.Cavicchi, M.Gaitan and Semancik, Tin oxide gas sensor fabricated using CMOS micro-hotplates and in-situ processing, *IEEE Electron Device Letters*, vol.14, no.3, pp.118-120, 1993.
- [6] N.R.Swart and A.Nathan, "Coupled electrothermal modeling of microheaters using SPICE", *IEEE Transactions on electron devices*, vol.41, no.6, pp.920-925.
- [7] R.E.Cavicchi, J.S.Suehle, K.G.Kreider, M. Gaitan and P.Chaparala, "Optimized temperature-pulse sequences for the enhancement of chemically specific response patterns from micro-hotplate gas sensors", *Sensors and Actuators B*, vol.33, pp.142-146, 1996.
- [8] W.-Y.Chung, J.-W.Lim, D.-D.Lee and N. Yamazoe, "Fabrication of low power micro-heater for micro-gas sensor - I. Thermal distribution analysis by finite element method", *J. Korean Sensor Society*, in contributed.
- [9] H.-S.Park et al., Tin oxide micro gas sensor for detecting  $\text{CH}_3\text{SH}$ , *Sensors and Actuators B*, vol.24-25, pp.478-481, 1995.

- [10] M.Ando, S.Suto, T.Suzuki, T.Tsuchida, C. Nakayama, N.Miura and N.Yamazoe, H<sub>2</sub>S-sensitive thin film fabricated from hydrothermally synthesized SnO<sub>2</sub> sol, J.Mater.Chem.,4(4)(1994)631-633.
- [11] DIN IEC 751(Deutsche Industrienorm).
- [12] V.Demarne and A.Grisel, An integrated low-power thin-film CO gas sensor on silicon, Sensors and Actuators,13(1988) 301-313.
- [13] I.Stoev and D.Kohl, An integrated gas sensor on silicon substrate with selective SnO<sub>x</sub> layer, Sensors and Actuators B2(1990)233-236.
- [14] W.-Y.Chung, T.-H.Kim, Y.-H.Hong and D.-D.Lee, Characterization of porous tin oxide thin films and their application to microsensor fabrication, Sensors and Actuators B24-25(1995)482-485.
- [15] D.-J.Yoo, J.Tamaki, S.J.Park, N.Miura and N.Yamazoe, Effects of thickness and calcination temperature on tin dioxide sol-derived thin-film sensor, J.Electrochem. Soc., 142(7)(1995) L105-L107.
- [16] J.W.Gardner, A.Pike, N.F.de Rooij, M. Koudelka-Hep, P.A.Clerc, A.Hierlemann, W.Göpel, Integrated arraysensor for detecting organic solvents, Sensors and Actuators B26-27(1995)135-139.

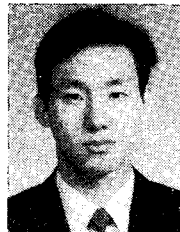
著 者 紹 介



정 완 영

1992년 8월 경북대학교 대학원 전자공학과 졸업(공학박사), 1993년 3월부터 세명대학교 전자공학과 조교수, 현재 일본 규슈대학교 재료개발공학과에 연구교수로 파견중임, 주관심분야 : 실리콘 마

이크로센서, 센서재료개발 등임.



장 동 근

1969년생. 1992년 경북대학교 전자공학과 졸업(공학사), 1994년 동대학원 전자공학과 졸업(공학석사), 1994년~현재 한국전자(주) 근무, 주관심분야 : 반도체 공정 및 가스센서

이 덕 동

『센서학회지 제1권 제1호』 논문 92-13, p. 116 참조.  
현재 경북대학교 전자·전기공학부 교수



이 상 문

1972년생. 1995년 경북대학교 전자공학과 졸업(공학사), 1997년 동대학원 전자공학과 졸업(공학석사), 1997년~현재 경북대학교 센서기술연구소.



노보루 야마조에

1968년 규슈대학교 대학원 공학연구과 박사과정수료(공학박사), 동대학 조수, 조교수를 거쳐 1981년부터 규슈대학 총합이공학연구과 재료개발공학전공 교수로 재직중. 주관심분야 : 반도체형 가스센서, ECD, 금속-공기전지 등의 기능성세라믹스.



강 봉 휘

1965년생. 1988년 경북대학교 전자공학과 졸업(공학사), 1991년 동대학원 전자공학과 졸업(공학석사), 1997년 동대학원 박사과정수료, 1996년 11월~현재 대구전문대학 전자과 전임강사.